Crossover SAFT Equation of State and Thermodynamic Properties of Propan-1-ol

S. B. Kiselev,[1,2] **J. F. Ely,**[1] **I. M. Abdulagatov,**[3,4] **and J. W. Magee**[3]

In this work we have developed a new equation of state (EOS) for propan-1-ol on the basis of the crossover modification (CR) of the statistical-associating-fluid-theory (SAFT) EOS recently developed and applied to *n*-alkanes. The CR SAFT EOS reproduces the nonanalytical scaling laws in the asymptotic critical region and reduces to the analytical-classical SAFT EOS far away from the critical point. Unlike the previous crossover EOS, the new CR SAFT EOS is based on the parametric sine model for the universal crossover function and is able to represent analytically connected van der Waals loops in the metastable fluid region. The CR SAFT EOS contains 10 system-dependent parameters and allows an accurate representation of the thermodynamic properties of propan-1-ol over a wide range thermodynamic states including the asymptotic singular behavior in the nearest vicinity of the critical point. The EOS was tested against experimental isochoric and isobaric specific heats, speed of sound, *PVT*, and VLE data in and beyond the critical region. In the one-phase region, the CR SAFT equation represents the experimental values of pressure with an average absolute deviation (AAD) of less than 1% in the critical and supercritical regions and the liquid densities with an AAD of about 1%. A corresponding states principle is used for the extension of the new CR SAFT EOS for propan-1-ol to higher *n*-alkanols.

---

[1] Chemical Engineering and Petroleum Refining Department, Colorado School of Mines, Golden, Colorado 80401-1887, U.S.A.

[2] To whom correspondence should be addressed. E-mail: skiselev@mines.edu.

[3] Physical and Chemical Properties Division, National Institute of Standards and Technology, Boulder, Colorado 80303, U.S.A.

[4] Guest scientist from Institute for Geothermal Problems of the Dagestan Scientific Center of the Russian Academy of Sciences, Kalinina Ave. 39-A, Makhachkala 367030, Dagestan, Russia.

1. INTRODUCTION

Since 1873, when van der Waals (vdW) first obtained an equation of state (EOS) that predicts a critical point and qualitatively explains the phase diagram of simple fluids [1], many attempts have been made to develop a thermodynamically consistent EOS for pure fluids. Starting in the 1940s a series of modifications of the two-parameter vdW EOS [2–4] was proposed to improve the cubic equation by incorporation of additional system-dependent parameters. More recently, three-, four-, and more parameter modifications of the vdW EOS have been proposed that yield better representations of the volumetric properties of simple fluids (see, e.g., Refs. 5–9). Although these modifications do improve the representation of the vapor pressure and single-phase densities of simple fluids, they generally do not improve the thermodynamic representation of complex materials such as polar, long-chain, polydisperse, and associating fluids [10, 11].

More modern molecular-based EOS such as the perturbed hard-sphere chain theory (PHSCT) [12–15] and the statistical associating fluid theory (SAFT) [16–21] models give better results for long-chain and associating fluids. However, even these theoretically based models are unable to reproduce simultaneously the heat capacities, speed of sound, *PVT*, and VLE data of pure fluids to within experimental accuracy. For this purpose empirical multiparameter BWR-type equations of state are usually used, which require very extensive experimental data sets in their development (for a review, see Ref. 22). At the present time, such wide-range data sets are available only for some technically important fluids such as water, carbon dioxide, light hydrocarbons, and a few others. For most of the fluids of interest in the chemical process industry, these extensive data sets are not available.

A fundamental problem appears when one applies any analytical EOS, molecular-based or empirical, for the prediction of the thermodynamic properties of fluids in the critical and supercritical region. The thermodynamics of a system in the critical region are dominated by the presence of long-range fluctuations in the density. As a consequence, the thermodynamic surface of fluids exhibits a singularity at the critical point which can be described in terms of nonanalytical scaling laws with universal critical exponents and universal scaling functions [23, 24]. All classical analytical EOS discussed above fail to reproduce the singular behavior of fluids in the critical region.

For an accurate representation of the near-critical thermodynamic surface of fluids, so-called asymptotic crossover models [25] can be used. The asymptotic crossover models incorporate scaling laws asymptotically close

to the critical point and are transformed into the analytical Landau expansion far away from the critical point. These crossover models can reproduce the thermodynamic properties of simple and complex fluids and fluid mixtures in the extended critical region to within experimental accuracy [26–42], but they cannot be extrapolated to low densities since they do not recover ideal gas behavior in the limit of zero density. Therefore, during the last two decades many efforts have been made to develop a crossover EOS that remains classical outside of the critical region but is transformed into the nonanalytical scaled EOS as the critical point is approached [43–62].

A general procedure for transforming any classical equation of state into a crossover EOS was recently proposed by Kiselev [63]. This procedure is based on the renormalization-group theory and is capable of accurately reproducing near-critical fluid behavior as well as correctly going to the ideal gas limit. In this paper we continue study of this model which was initiated by Kiselev and co-workers for the cubic [63, 64] and SAFT [65–67] EOS. Using the simplified crossover SAFT EOS obtained earlier for *n*-alkanols [67], we develop a new crossover SAFT EOS for propan-1-ol. The new equation of state was tested against an extensive set of experimental data for the volumetric and caloric properties of propan-1-ol in both the one- and the two-phase regions. In testing the CR SAFT EOS in the critical region, new experimental data for the isochoric heat capacity for propan-1-ol were used. Unlike the simplified SAFT model [67], which focused on the representation of volumetric properties and phase equilibria, the new crossover SAFT EOS also reproduces the scaling behavior of the isochoric heat capacity and speed of sound in the asymptotic critical region.

2. CROSSOVER SAFT EQUATION

To obtain a crossover formulation of the SAFT EOS, one needs to start from the classical equation of state. In this work, for the classical SAFT EOS we adopt the model developed by Huang and Radosz [17] as represented in crossover form by Kiselev and Ely [65, 66]. Following our previous work, we represent the dimensionless crossover Helmholtz free energy $\bar{A}(T, v) = a(T, V, N)/RT$ for the SAFT equation in the form

$$\bar{A}(T, v) = \Delta\bar{A}(\bar{\tau}, \Delta\bar{\eta}) - P_0(T)\,\Delta v + \bar{A}_0(T) - \mathrm{K}(\tau^2) \tag{1}$$

where $\tau = T/T_c - 1$ is the dimensionless deviation of the temperature T from the critical temperature T_c, $\Delta\eta = \Delta v/v_c = v/v_c - 1$ is the dimensionless deviation of the molar volume $v = V/N$ from the critical volume v_c, and $\bar{\tau}$

and $\Delta\bar{\eta}$ are their renormalized values, specified below. The critical part of the dimensionless Helmholtz free energy is

$$\Delta\bar{A}(\bar{\tau}, \Delta\bar{\eta}) = \bar{A}^{res}(\bar{\tau}, \Delta\bar{\eta}) - \bar{A}^{res}(\bar{\tau}, 0) + \bar{P}_0(\bar{\tau})\,\Delta\bar{\eta} - \ln(\Delta\bar{\eta} + 1) \tag{2}$$

where the dimensionless residual part of the Helmholtz free energy $\bar{A}^{res} = a^{res}/RT$ is given by

$$\bar{A}^{res}(\bar{\tau}, \Delta\bar{\eta}) = m\left[\frac{4\bar{\eta} - 3\bar{\eta}^2}{(1 - \bar{\eta})^2} + \sum_i \sum_j D_{ij}\left(\frac{u}{kT_{0c}(\bar{\tau} + 1)}\right)^i \left(\frac{\bar{\eta}}{\eta_0}\right)^j\right]$$
$$+ (1 - m) \ln g^{hs}(\bar{\eta}) + \bar{A}^{assoc}(\bar{\tau}, \Delta\bar{\eta}) \tag{3}$$

where m is the number of monomer segments in the molecule and the D_{ij} are universal constants [68].

$$g^{hs}(\bar{\eta}) = \frac{2 - \bar{\eta}}{2(1 - \bar{\eta})^3} \tag{4}$$

is the hard-sphere radial distribution function at contact, $\bar{\eta} = \eta_{0c}/(\Delta\bar{\eta} + 1)$ is the renormalized reduced density, $\eta_{0c} = \eta_0 m v^0/v_{0c}$ is the reduced critical density, and $\eta_0 = 0.74048$. The dimensionless crossover Helmholtz free energy change due to association, the last term in Eq. (3), is given by [67]

$$\bar{A}^{assoc}(\bar{\tau}, \Delta\bar{\eta}) = \sum_A \left(\ln X^A - \frac{X^A}{2}\right) + \frac{1}{2}M \tag{5}$$

where M is the number of association sites and X^A is the mole fraction of molecules not bonded at site A, which is calculated from

$$X^A = \left(1 + N_A \sum_B X^B \Delta^{AB}\right)^{-1} \tag{6}$$

where the sum runs over all bonding sites and

$$\Delta^{AB} = \kappa^{AB} \frac{6\eta_0 v^{00}}{\pi N_A}\left[\exp(\varepsilon^{AB}/kT_{0c}(\bar{\tau} + 1) - 1\right] g^{hs}(\bar{\eta}) \tag{7}$$

In Eqs. (3)–(7), N_A is Avogadro's number, R is the universal gas constant, k is the Boltzmann constant, and the parameters v^0 and u are given by

$$v^0 = v^{00}\left[1 - C\exp\left(\frac{-3u^0}{kT_{0c}(\bar{\tau} + 1)}\right)\right]^3 \tag{8}$$

$$u = u^0\left(1 + \frac{e}{kT_{0c}(\bar{\tau} + 1)}\right) \tag{9}$$

where $C = 0.12$, $e/k = 10$, and v^{00}, u^0, ε^{AB}, and κ^{AB} are system-dependent parameters. In Eqs. (3)–(9), the parameters T_{0c} and v_{0c} are the classical critical parameters of the original SAFT EOS, which depend on the parameters m, v^{00}, u^0, ε^{AB}, and κ^{AB} and can be found from the numerical solutions of the equations

$$P_{0c} = -\left(\frac{\partial a}{\partial v}\right)_{T_{0c}}, \qquad \left(\frac{\partial^2 a}{\partial v^2}\right)_{T_{0c}} = 0, \qquad \left(\frac{\partial^3 a}{\partial v^3}\right)_{T_{0c}} = 0 \qquad (10)$$

The dimensionless residual part of the Helmholtz free energy on the critical isochore is

$$\bar{A}^{res}(\bar{\tau}, 0) = m\left[\frac{4\eta_{0c} - 3\eta_{0c}^2}{(1 - \eta_{0c})^2} + \sum_i \sum_j D_{ij}\left(\frac{u}{kT_{0c}(\bar{\tau} + 1)}\right)^i \left(\frac{\eta_{0c}}{\eta_0}\right)^j\right]$$
$$+ (1 - m)\ln g^{hs}(\bar{\eta}) + \bar{A}^{assoc}(\bar{\tau}, 0) \qquad (11)$$

and the renormalized pressure is given by [65]

$$\bar{P}_0(\bar{\tau}) = m\left[\frac{4\eta_{0c} - 2\eta_{0c}^2}{(1 - \eta_{0c})^3} + \sum_i \sum_j jD_{ij}\left(\frac{u}{kT_{0c}(\bar{\tau} + 1)}\right)^i \left(\frac{\eta_{0c}}{\eta_0}\right)^j\right]$$
$$+ (1 - m)\frac{5\eta_{0c} - 2\eta_{0c}^2}{(1 - \eta_{0c})(2 - \eta_{0c})} - \sum_A \left(\frac{1}{X^A} - \frac{1}{2}\right)\left(\frac{\partial X^A}{\partial \Delta\bar{\eta}}\right)_{\bar{\tau}(\Delta\bar{\eta} = 0)} \qquad (12)$$

The temperature-dependent functions $\bar{A}_0^r(T)$ and $\bar{P}_0(T)$ in Eq. (1) are given by

$$\bar{A}_0^{res}(T) = m\left[\frac{4\eta_{0c} - 3\eta_{0c}^2}{(1 - \eta_{0c})^2} + \sum_i \sum_j D_{ij}\left(\frac{u}{kT}\right)^i \left(\frac{\eta_{0c}}{\eta_0}\right)^j\right]$$
$$+ (1 - m)\ln g^{hs}(\eta_{0c}) + \bar{A}^{assoc}(T, g^{hs}(\eta_{0c})) \qquad (13)$$

$$\bar{P}_0(T) = m\left[\frac{4\eta_{0c} - 2\eta_{0c}^2}{(1 - \eta_{0c})^3} + \sum_i \sum_j jD_{ij}\left(\frac{u}{kT_{0c}(\bar{\tau} + 1)}\right)^i \left(\frac{\eta_{0c}}{\eta_0}\right)^j\right]$$
$$+ (1 - m)\frac{5\eta_{0c} - 2\eta_{0c}^2}{(1 - \eta_{0c})(2 - \eta_{0c})} - \sum_A \left(\frac{1}{X^A} - \frac{1}{2}\right)\left(\frac{\partial X^A}{\partial \eta_{0c}}\right)_{T(\bar{\eta} = \eta_{0c})} \qquad (14)$$

where the hard-sphere distribution function $g^{hs}(\eta_{0c})$ is given by Eq. (4) with $\bar{\eta} = \eta_{0c}$, and parameters v^0 and u are given by Eqs. (8) and (9). Equations (11) and (12), and Eqs. (13) and (14), have similar forms, and the principal

difference between them is in the argument of the functions $\bar{A}_0^{res}$ and $\bar{P}_0$. In Eqs. (13) and (14), $\bar{A}_0^{res}$ and $\bar{P}_0$ are functions only of the temperature T, while $\bar{A}_0^{res}$ and $\bar{P}_0$ as given by Eqs. (11) and (12) are functions of the renormalized temperature $\bar{\tau}$, which depends on both variables, T and v.

The renormalized temperature $\bar{\tau}$ and order parameter $\Delta\bar{\eta}$ in Eqs. (1)–(2) are defined in terms of the real dimensionless temperature τ and the real order parameter $\Delta\eta$ through

$$\bar{\tau} = \tau \mathrm{Y}^{-\alpha/2\varDelta_1} + (1 + \tau)\, \Delta\tau_c\, \mathrm{Y}^{2(2-\alpha)/3\varDelta_1} \tag{15}$$

$$\Delta\bar{\eta} = \Delta\eta\, \mathrm{Y}^{(\gamma-2\beta)/4\varDelta_1} + (1 + \Delta\eta)\, \Delta\eta_c\, \mathrm{Y}^{(2-\alpha)/2\varDelta_1} \tag{16}$$

where the factors $\Delta\tau_c = (T_c - T_{0c})/T_{0c}$ and $\Delta\eta_c = (v_c - v_{0c})/v_{0c}$ are the dimensionless shifts of the real critical temperature T_c and the real critical volume v_c from the classical equation of state values, T_{0c} and v_{0c}.

The kernel term in Eq. (1) can be written

$$\mathrm{K}(\tau^2) = \tfrac{1}{2} a_{20} \tau^2 (\mathrm{Y}^{-\alpha/\varDelta_1} - 1) + \tfrac{1}{2} a_{21} \tau^2 (\mathrm{Y}^{-(\alpha-\varDelta_1)/\varDelta_1} - 1) \tag{17}$$

where the first term corresponds to the asymptotic limit and the second term to the first Wegner correction for the isochoric specific heat on the critical isochore [69]. In Eqs. (15)–(17), $\gamma = 1.24$, $\beta = 0.324$, $\alpha = 2 - \gamma - 2\beta = 0.110$, and $\varDelta_1 = 0.51$ are the universal nonclassical critical exponents. The crossover function Y in Eqs. (15)–(17) is represented in the parametric form [65, 66]

$$\mathrm{Y} = \left(\frac{q}{1+q}\right)^{2\varDelta_1} \tag{18}$$

which in the first order of an ε-expansion, corresponds to the crossover function obtained by Belyakov et al. [42] for the crossover Leung–Griffiths model.

In Eq. (18), the parametric variable $q^2 = r/Gi$, where r has the meaning of a dimensionless measure of the distance from the critical point, and the system-dependent parameter Gi is the Ginzburg number [63]. In our previous work [63–65], the variable r was found from a solution of the parametric linear model (LM) EOS. In the present work, following Kiselev et al. [66, 67], we find the parametric variable r from a solution of the parametric sine model (SM) developed recently by Fisher and co-workers [70]. In the one-phase region, the LM and SM are physically equivalent. However, unlike the LM, the SM can be extended into the metastable region and can represent analytically connected van der Waals loops.

Finally, the parametric variable q in the sine model is determined from the solution of the equation [66]

$$\left(q^2 - \frac{\tau}{Gi}\right)\left[1 - \frac{p^2}{4b^2}\left(1 - \frac{\tau}{q^2 Gi}\right)\right]$$

$$= \frac{b^2}{Gi^{2\beta}}\left(\frac{q}{1+q}\right)^{2(1-2\beta)} \times \left\{\Delta\eta[1 + v_1 \Delta\eta^2 \exp(-\delta_1 \Delta\eta)] + d_1\tau(1 - 2\tau)\right\}^2 \tag{19}$$

where $\delta_1 = 8.5$, and the parameters p^2 and b^2 can be set equal to the universal LM model parameter, $p^2 = b^2 = b_{LM}^2 = 1.359$ [66]. The linear-model crossover equation employed earlier by Kiselev et al. [63–65] for the parametric variable q is recaptured from Eq. (19) when the parameter $p^2 \to 0$.

The crossover SAFT equation of state can be obtained from the crossover expression, Eq. (1), by differentiation with respect to volume

$$P(T, v) = \frac{RT}{v_{0c}}\left[-\frac{v_{0c}}{v_c}\left(\frac{\partial\Delta\bar{A}}{\partial\Delta\eta}\right)_T + \bar{P}_0(T) + \frac{v_{0c}}{v_c}\left(\frac{\partial K}{\partial\Delta\eta}\right)_T\right] \tag{20}$$

3. EXPERIMENTAL DATA FOR PROPAN-1-OL

3.1. *PVT* Data

Five major data sets of *PVT* measurements are available for propan-1-ol [71–75]. Golubev et al. [72] reported data obtained using a modified hydrostatic weighing method in the temperature range 290 to 620 K with pressures up to 50 MPa. The uncertainty of these density measurements is 0.1% in the range far from the critical point, increasing to 0.2% in the critical region. The uncertainty in pressure is 0.05%, while for temperature measurements it is 2 mK. These data differ from the earlier data of Golubev and Bagina [73] by up to 1%.

A constant volume method was used by Tseng and Stiel [74] for density measurements in the temperature range between 473 and 623 K at pressures between 6.8 and 54.4 MPa. The uncertainty of these measurements is 0.4 to 0.5%. There are differences of up to 1.5% between the measurements reported in Refs. 72 and 73, but some of the data points show deviations of up to 4%. Extensive *PVT* measurements for vapor and liquid propan-1-ol in the temperature range from 303 to the critical temperature, 536.75 K, and pressures up to 70 bar were also made by Ramsay and

Young [71]. The scatter around average values of these data is about 1%. Low-temperature (between 140 and 370 K and at pressures up to 70 MPa) measurements of PVT properties for propan-1-ol have been reported by Zakar'yaev [75]. The uncertainty of these density measurements is 0.05%.

3.2. Experimental Heat Capacity and Speed-of-Sound Data

Only two data sets [75, 76] are available for C_V of propan-1-ol. The isochoric heat capacity data for propan-1-ol at temperatures from 149 to 358 K along eight liquid isochores, including both the one- and the two-phase regions were reported by Zakar'yaev [75], who used a compensation-relaxation method. The uncertainty of these measurements is 0.7%. A total of 950 values of C_V for propan-1-ol was reported along 32 liquid and vapor isochores between 67 and 777 kg·m^{-3} by Amirkhanov et al. [76], who used a high-temperature, high-pressure integrating adiabatic calorimeter in their study. For each liquid or vapor isochore, the C_V measurements were made in the one- and two-phase regions, including liquid, vapor, subcritical, and supercritical states. Around the phase transition temperature, data were measured in more detail to determine more accurately the saturation densities and temperatures on the coexistence curve. For all measured isochores, the values of both the phase transition temperature T_S and the one-(C_{V1}) and two-phase phase heat capacity (C_{V2}) at saturation are reported in this paper. In general, the uncertainty of the heat capacity is 0.3–1.0% in the liquid phase, 1–3.5% in the vapor phase, and 2–3.5% near the critical point.

All available measurements of the isobaric heat capacity C_P and sound velocity W data for propan-1-ol at atmospheric pressure from a temperature of 146 K up to 370.35 K have been analyzed and correlated by Khasanshin [77]. At elevated pressures, most of the available data for isobaric heat capacity C_P of propan-1-ol cover the temperature range from 154 to 361 K [78–81]. Data between 293 and 473 K and at pressures up to 16 MPa were reported by Yanin [82] and Grigor'ev et al. [83] using an adiabatic calorimeter. The accuracy of these measurements is 0.9%. Mathews and McKetta [84] and Sinke and Vries [85] also measured the isobaric heat capacity of propan-1-ol in the temperature range from the normal boiling point to 451 K at low pressures (about atmospheric pressure, 0.1 MPa) using a flow calorimeter. The uncertainty of the Sinke and Vries [85] data is about 4 J·mol^{-1}.

The most reliable sound velocity data for propan-1-ol are reported in Refs. 86–91. The uncertainty of measurements by Emery et al. [87] and Gasse and Emery [88] is about 0.01%. Agreement within 0.08% is found between Emery et al. [87] and Gasse and Emery [88]. Wilson and

Bradley [86] have measured the sound velocity of propan-1-ol for temperatures and pressures in the ranges $273 < T < 333$ K and $0.1 < P < 96.5$ MPa. Hagelberg [89] measured the sound velocity in propan-1-ol at a temperature of 303 K and at pressures up to 1000 MPa. The accuracy of these data is better than 0.25%. The values of sound velocity in propan-1-ol reported by Wilson and Bradley [86] at atmospheric pressure differ from the Hagelberg [89] results by 1 to 1.5 m·s^{-1} (0.084 to 0.13%), and they differ from the results of Carnevale and Litovitz [90] by 1%. Sysoev et al. [91] reported sound velocity and derived thermodynamic data for proponal-1-ol in the temperature range from 293 to 353 K and at pressures up to 850 MPa. The uncertainty of these data is about 0.05 to 0.2%.

3.3. Experimental Data at the Saturation Curve

Experimental data for propan-1-ol on the coexistence curve are relatively scarce. Amirkhanov et al. [76] reported experimental temperature T_S, density ρ_S, liquid-phase, vapor-phase and two-phase isochoric heat capacity (C_{V1}, C_{V2}) measurements and derived thermodynamic properties including isobaric heat capacity C_P and speed of sound W in the temperature range from 273.15 K to the critical point ($T_c = 536.56$ K). Saturated-liquid and -vapor density data for propan-1-ol have been reported [72, 75, 78, 80, 92–102]. Saturated-liquid and -vapor volumes were measured by Ramsay and Young [71] between 273 K and the critical point for liquid and from 353 K to the critical temperature for vapor. Ambrose and Townsend [92] report saturated-liquid density data in the temperature range from 414.8 K to the critical point which show good agreement ($<0.5\%$) with the results of Ramsay and Young [71]. At temperatures above 353 K, the differences between these two data sets are typically less than 0.2%, but their low-temperature saturated-vapor volumes are significantly different (by about 10%). Near the critical point, the deviations are about 0.5%, which is close to the uncertainty claimed by the authors. Hales and Ellender [95] measured liquid density at saturation in the temperature range from 293 to 490 K by means of a magnetically controlled float that could be held in the center of the sample, with the sample cell suspended from an automatic balance. The accuracy of this data set is about ± 0.15 kg·m^{-3}. These data at low temperatures (293 to 298 K) are lower than values selected by Wilhoit and Zwolinski [78] by 0.2 to 0.4 kg·m^{-3}. In the temperature range from 415 to 480 K, the disagreement reaches $\pm(2$ to $3)$ kg·m^{-3} (0.25 to 0.35%) with data reported by Young [103], Dannhauser and Bahe [98], and Ambrose and Townsend [92]. Most of the data show good agreement with each other except [80, 104] in the critical region, especially in the vapor phase. Cibulka [105] critically

evaluated the available experimental data for saturated liquid density in the temperature range from 153 to 529.8 K and proposed a correlating equation. The uncertainty of the recommended values of saturated liquid density near the critical point is about 1 kg · m^{-3} (about 0.4%) or more. Rathmann et al. [106] also recommended vapor and liquid saturated data for propan-1-ol on the basis of a detailed analysis of available data.

Vapor pressures for propan-1-ol have been measured by several authors [71, 92, 107]. Ambrose and Townsend [92] reported vapor pressure data in the temperature range from 405.5 K to the critical point (536.71 K) with an uncertainty of about 0.004 bar. Ramsay and Young [71] measured vapor pressures in the temperature range from 353 K to the critical point (536.85 K), with their results being about 1% lower than those of Ambrose and Townsend [92] and Biddiscombe et al. [107]. The agreement between Ambrose and Townsend [92] and Bidsdiscombe et al. [107] was found to be within the combined experimental uncertainty claimed by the authors. Efremov [93] measured the vapor pressure for propan-1-ol in the temperature range from 343 to 533 K. Ambrose and Walton [108] reported a vapor-pressure equation based on selected experimental data. A comprehensive list of references for the relevant experimental vapor-pressure data may be found in Ref. 109.

Counsell et al. [110] reported 48 data points for C_P at saturation in the temperature range from 153.9 to 361.5 K with an estimated uncertainty of about 0.1 to 0.15%. Yanin [82] measured C_P along the coexistence curve in the temperature range from 293 to 473 K with an accuracy of 0.9%. Low-temperature (from 150 to 360 K) measurements of C_P have been made by Zakar'yaev [75]. C_P values derived from isochoric heat capacity and sound velocity data for propan-1-ol are reported in Refs. 76 and 111.

The sound velocity at saturation was measured by Timofeev and Alekseev [111] in the temperature range from 153 to 333 K with an uncertainty of 0.2%. These authors also reported saturated thermodynamic properties (C_V, C_P) of propan-1-ol derived from sound velocity data.

3.4. Critical Parameters

The available literature data on critical constants of propan-1-ol are given in Table I. The values of T_c, ρ_c, and P_c reported for propan-1-ol differ by about 0.74 K, 7.1 kg · m^{-3}, and 0.17 MPa. These data have been obtained by a variety of experimental methods and procedures including the following:

(1)   disappearance of the meniscus (usually the average value of the temperatures of disappearance and reappearance of the meniscus),

Table I. Reported Values of the Critical Properties of Propan-1-ol

T_c (K)	P_c (MPa)	ρ_c (kg·m^{-3})	Ref. No.
536.85	5.083	280.0	71
537.25	—	—	122
537.25	—	—	123
537.30	5.087	273.1	124
536.85	—	—	96
536.71	5.170	275.4	92
537.15	5.168	273.0	93
537.25	5.218	—	125
536.75	5.168	—	126
536.56	5.170	272.9	76
536.71	5.170	275.0	78
536.85	5.083	273.4	103
536.71	5.170	275.4	115
536.78	5.168	274.0	108
536.95	5.155	278.0	97
537.15	5.088	273.0	127
536.78	—	275.0	95
536.84	5.075	273.4	112
537.04	5.088	272.9	99
537.30	5.087	273.2	128
536.71	5.170	275.0	114
536.85	5.168	273.0	80
536.84	5.075	273.4	104
537.22	5.047	—	125
536.85	5.050	—	83
536.85	5.083	273.4	129

(2) disappearance of the meniscus upon a very slight volume increase (pressure decrease),

(3) the law of rectilinear diameters,

(4) *PVT* relations, $(\partial P/\partial V)_T = 0$, and

(5) the method of quasi-static thermograms.

Ambrose and Townsend [112] used a visual method for measurement of T_c. Pressure was determined while the disappearance and reappearance of the meniscus were observed visually. The critical temperature T_c and critical pressure P_c were obtained simultaneously in this way. The critical density ρ_c was obtained by application of the law of rectilinear diameters of the orthobaric densities $\rho_d = (\rho_l + \rho_g)/2$ measured over a range of temperatures. The approximately linear relation between $(\rho_l - \rho_g)$ and $\tau^{1/3}$ was demonstrated. However, the coexistence curve shape near the critical point

shows some peculiarities. In particular, according to the modern theory of liquid–gas critical phenomena [113], the first temperature derivative $d\rho_d/dT$ of the coexistence-curve diameter ρ_d diverges in a manner similar to the isochoric heat capacity $\tau^{-\alpha}$. That is, as the reduced temperature τ goes to zero, the diameter varies as

$$\rho_d = \rho_c + B_2 |\tau|^{1-\alpha} + B_3 \tau + \cdots \qquad (21)$$

where $\alpha = 0.112$ is the exponent that describes the behavior of the isochoric heat capacity; B_3 is the amplitude of the rectilinear diameter of the coexistence curve. The second term in Eq. (21), $\sim |\tau|^{1-\alpha}$, corresponds to the "singular diameter law" and the third term, linear in τ, corresponds to the "rectilinear diameter law." Experimental $T_S-\rho_S$ data on the coexistence curve derived from an isochoric heat capacity experiment confirmed the validity of the basic idea of the renormalization group theory [113]. Figure 1 shows a plot of the diameter data of propan-1-ol as a function of temperature T. Some data sets, for example, those of Loktev [80] and Martin et al. [104], exhibit significant deviations from straight lines in the temperature range where $|\tau| < 2.5 \times 10^{-3}$. The data of Amirkhanov et al. [76], Efremov [93], Cosner et al. [99], and Rathmann et al. [106] show good agreement with the singular diameter law predicted by renormalization group theory [113]. It is evident from Fig. 1 that near the critical point, the diameter behavior differs from the "rectilinear diameter law" and is also
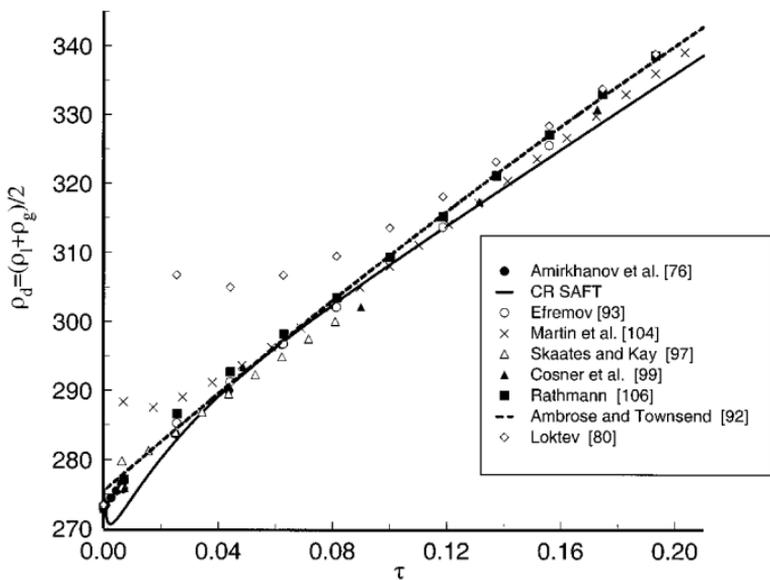
Fig. 1. The rectilinear diameter of the coexistence curve for propan-1-ol from various experimental and calculated data.

characterized by the term $\sim |\tau|^{1-\alpha}$. Therefore, a simple linear extrapolation of the diameter of the coexistence curve to the critical point, at $\tau \to 0$, without taking into account the "singular diameter" term, can give rise to an uncertainty of the determination of the critical density of up to 2 to 3%.

Young [103] used Methods 2 and 3 for determination of the critical properties to obtain a T_c whose accuracy is ± 0.1 K. There is good agreement between the values of T_c found in Refs. 103 and 112, but the P_c values differ by almost 1 bar. Kay and Donham [114] used Methods 3 and 4 for measurements of critical properties, and their results show satisfactory agreement with Ambrose's results for all three critical properties. However, values of critical parameters recommended by Kubicek and Eubank [115] differ considerably from these values.

The disappearance of the meniscus method was used by Skaates and Kay [97] for measurement of the critical temperature and critical pressure of propan-1-ol. The value of the critical density was obtained by the application of the "law of the rectilinear" diameter. The accuracy of the measurements are as follows: T_c, ± 0.22 K; P_c, ± 0.0069 MPa; and ρ_c, ± 3 kg·m^{-3}.

The method of quasi-static thermograms was used by Amirkhanov et al. [76] for measurements of the saturation temperatures and densities near the critical point. A thermogram is a plot of temperature T versus time τ while a sample is continuously heated or cooled. This method is quite accurate for measurements of the critical properties of fluids (critical temperature, ± 0.02 K; critical density, $\pm 0.15\%$) and has some advantages compared with conventional methods. On intersecting the phase transition curve, the heat capacity is known to change discontinuously, leading to a sharp (20–30%) change in the thermogram slope $(dT/d\tau)$, thereby giving a precise definition of the phase transition point. In contrast, the method of determining parameters of the coexistence curve by the meniscus disappearance lacks objectivity. The visual observation of the meniscus becomes less and less reliable as the critical point is approached. In addition, the observations are impeded by the development of critical opalescence. Therefore, the region of temperatures (about ± 0.1 K) around the critical point becomes virtually unattainable for investigation. The method of quasi-static thermograms makes it possible to obtain reliable data at temperatures in a region very close to $T_c \pm 0.01$ K.

Values of critical temperature and critical density derived from calorimetric measurements using the method of quasi-static thermograms by Amirkhanov et al. [76] are $T_c = 536.56$ K and $\rho_c = 272.9$ kg·m^{-3}. These critical parameters show satisfactory agreement (within $\pm 0.15\%$) with other reliable data (see Table I). The critical pressure was found by numerical integration of a differentiated form of the Clapeyron equation combined with

the Yang–Yang [116] relation. The values of these parameters calculated for propan-1-ol are $P_c = 5.184$ MPa and $(dP_S/dT)_c = 0.0792$ MPa · K^{-1}. These values are in good agreement with those obtained from the Kubicek and Eubank [115] correlation ($P_c = 5.17$ MPa and $(dP_S/dT)_c = 0.0799$ MPa · K^{-1}).

Finally, the values

$$T_c = 536.71 \pm 0.1 \text{ K}, \qquad P_c = 5.184 \pm 0.01 \text{ MPa}, \qquad \text{and}$$
$$\rho_c = 273.2 \pm 0.31 \text{ kg} \cdot \text{m}^{-3} \tag{22}$$

are the recommended critical parameters for propan-1-ol.

4. EQUATION OF STATE FOR PROPAN-1-OL

The crossover SAFT EOS contains the following system-dependent parameters: the original SAFT parameters, m, v^{00}, u^0, ε^{AB}, and κ^{AB}, and the crossover parameters, Gi, d_1, v_1, a_{20}, and a_{21}. As pointed out above [see Eq. (10)], the parameters m, v^{00}, u^0, ε^{AB}, and κ^{AB} determine the classical values of the critical parameters for the SAFT EOS, which in general do not coincide with the experimental values. Therefore, if one wants to keep the experimental values of the critical temperature T_c and density ρ_c, they should be considered to be additional system-dependent constants. Here, for T_c and ρ_c we adopt the recommended values listed above. Unlike the critical temperature and density, the critical pressure P_c in the CR SAFT EOS is determined by all parameters T_c, ρ_c, m, v^{00}, u^0, ε^{AB}, and κ^{AB} and cannot be set equal to the experimental value.

The Ginzburg number, Gi, and the critical amplitudes a_{20} and a_{21} in Eq. (17) determine the crossover behavior of the isochoric heat capacity along the critical isochore and can be determined independently from the other parameters. Here we found these parameters from a fit of the CR SAFT EOS to the experimental C_V data obtained on the near-critical isochores of Amirkhanov et al. [76] with the parameters m, v^{00}, u^0, ε^{AB}, κ^{AB}, d_1, and v_1 obtained earlier for propan-1-ol in the simplified CR SAFT model [67]. After that, the parameters m, v^{00}, u^0, ε^{AB}, κ^{AB}, d_1, and v_1 were found from a fit of the crossover SAFT EOS to the experimental saturated pressure, VLE, and one-phase PVT data [93, 117, 118] with the fixed values of the parameters Gi, a_{20}, and a_{21}. The values of all system-dependent parameters for the CR SAFT EOS are listed in Table II, and the critical parameters are given in Table III. The values of the critical pressure, $P_c = 5.17$ MPa, and of the slope of the vapor pressure curve at the critical point, $(dP_S/dT)_c = 0.0787$ MPa · K^{-1}, calculated with the CR SAFT EOS with parameters given in Table II, are in good agreement with the experimental values.

Table II. System-Dependent Constants of the CR SAFT EOS for Propan-1-ol

SAFT parameters		Crossover parameters	
Parameter	Value	Parameter	Value
v^{00} (ml·mol^{-1})	8.1327	Gi	0.109967
M	5.0537	d_1	1.58296
u^0/k (K)	179.99	v_1	0.01969
ε^{AB}/k (K)	2418.1	a_{20}	20.4118
κ^{AB}	0.0474	a_{21}	-1.0609

5. COMPARISON WITH EXPERIMENTAL DATA

The CR SAFT EOS was compared to available experimental thermo-dynamic data (PVT, C_V, C_P, and W) for propan-1-ol. Comparisons of the calculated isochoric heat capacity with experimental data measured by Amirkhanov et al. [76] in both the critical and the supercritical regions are shown in Fig. 2. Deviation plots for the experimental data are given in Fig. 3. All near-critical isochores show satisfactory agreement with values calculated from CR SAFT in the one-phase region. Excellent agreement was found for near-critical isochores of 309.5, 323.6, and 344.2 kg·m^{-3}. The average absolute deviations (AAD) for these isochores are about 1.5%. Relatively large deviations (8 to 11%) were found for isochores at 255.2, 217.1, and 285.2 kg·m^{-3} in the immediate vicinity of the phase transition point. Most of the data show systematic deviations. Systematically

Table III. Critical Parameters and Acentric Factors for *n*-Alkanols

					ω	
Fluid	T_c (K)	ρ_c (mol·L^{-1})	P_c (MPa)	M_w	Ref. 11	Ref. 108
Propan-1-ol (this work)	536.71	4.583	5.170	60.097	0.624	0.620
Butan-1-ol [130]	562.90	3.650	4.418	74.123	0.590	0.591
Pentan-1-ol [131]	588.15	3.030	3.911	88.150	0.580	0.579
Hexan-1-ol [132]	611.40	2.625	3.510	102.177	0.560	0.575
Heptan-1-ol [132]	633.15	2.298	3.121	116.204	0.560	0.580
Octan-1-ol [93]	658.15	2.043	2.988	130.231	0.530	0.594
Nonan-1-ol [93]	683.15	1.837	2.675	144.26	0.525[a]	0.610
Decan-1-ol [93]	708.15	1.667	2.533	158.39	0.484[a]	0.629

[a] Estimate based on the experimental data presented in Fig. 17.
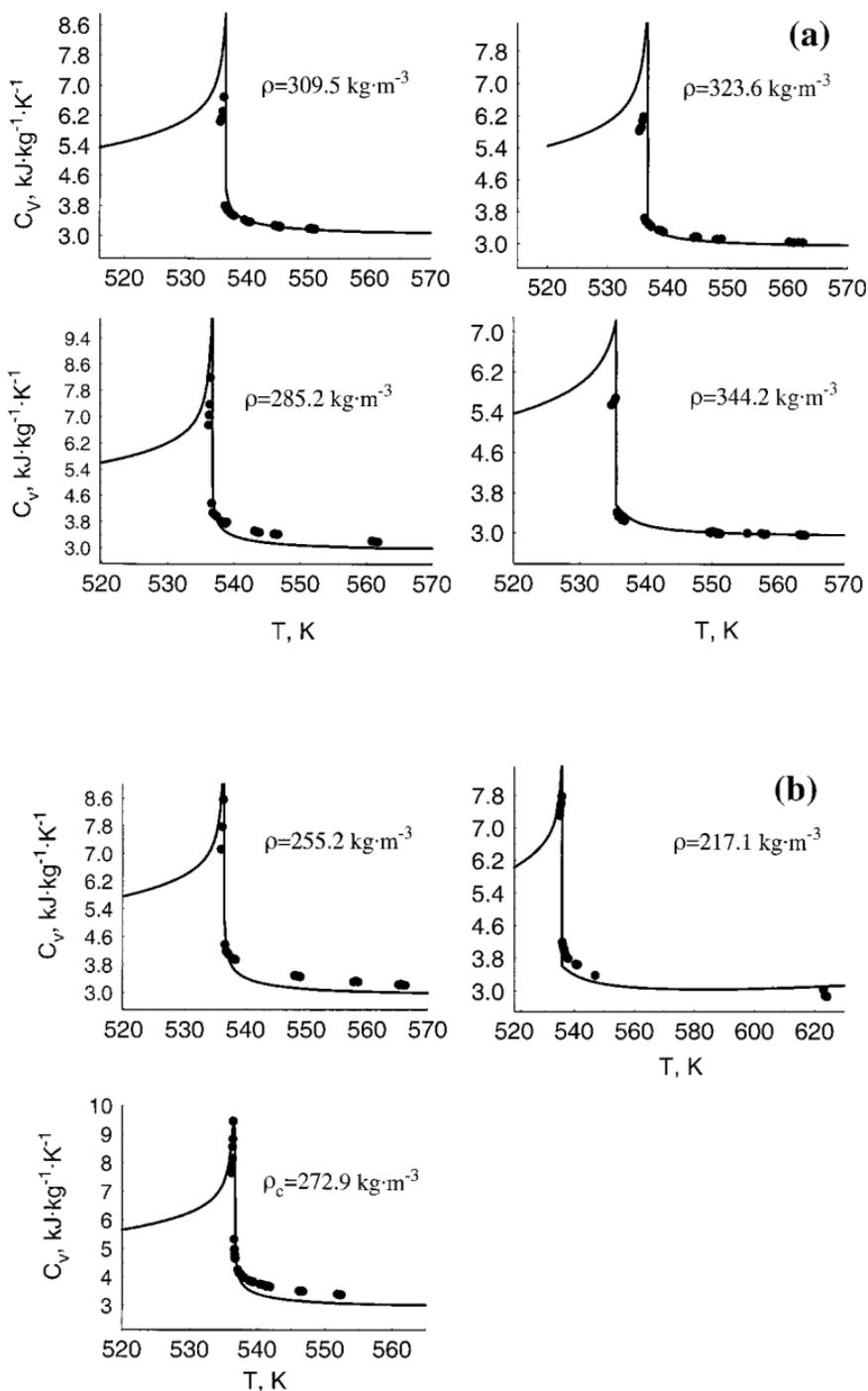
Fig. 2. Experimental one-phase and two-phase isochoric heat capacity of propan-1-ol as a function of temperature along the near-critical densities together with values calculated with CR SAFT EOS.
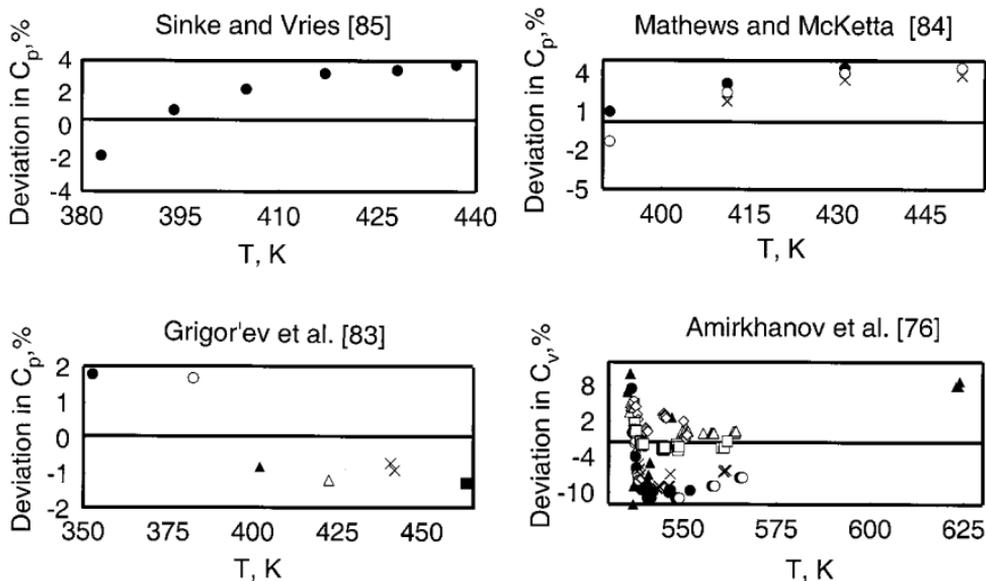
Fig. 3. Percentage deviations of isochoric and isobaric heat capacities of propan-1-ol by various authors with the values calculated with CR SAFT EOS. Sinke and Vries [85] ($\bullet$, 0.1 MPa); Mathews and McKetta [84] ($\bullet$, 0.1 MPa; $\bigcirc$, 0.135 MPa; $\times$, 0.169 MPa); Grigor'ev et al. [83] ($\blacksquare$, 15.2 MPa; $\times$, 11.0 MPa; $\triangle$, 7.85 MPa; $\bullet$, 2.15 MPa; $\bigcirc$, 3.9 MPa; $\blacktriangle$, 5.85 MPa); Amirkhanov et al. [76] ($\blacktriangle$, 217.1 kg $\cdot$ m^{-3}; $\bigcirc$, 255.2 kg $\cdot$ m^{-3}; $\square$, 323.6 kg $\cdot$ m^{-3}; $\triangle$, 344.2 kg $\cdot$ m^{-3}; $\times$, 285.2 kg $\cdot$ m^{-3}; $\bullet$, 272.9 kg $\cdot$ m^{-3}; $\diamond$, 309.5 kg $\cdot$ m^{-3}).

large deviations of about 24% were observed for the two-phase region in the immediate vicinity of a phase transition temperature. Good agreement was found for the isochoric heat capacity in both the one- and the two-phase regions on the critical isochore $\rho = 272.9$ kg $\cdot$ m^{-3} (see Fig. 2b).

In Fig. 4 we show a comparison of the experimental and calculated isochoric heat capacity for propan-1-ol in the supercritical region. Comparisons of the experimental and calculated values of the one-phase (C_{V1}) and two-phase (C_{V2}) isochoric heat capacities at saturation are depicted in Figs. 5 and 6. From these figures, one can see that the CR SAFT prediction of the C_V at saturation is in satisfactory agreement with the experimental data of Amirkhanov et al. [76], but small systematic disagreement is seen in the temperature range where C_{V1} and C_{V2} display an anomaly when compared with typical fluid behavior. This problem needs special study to develop an improved form of the CR SAFT.

Deviations between experimental and calculated isobaric heat capacity of propan-1-ol are given in Fig. 3. Excellent agreement (within 2%) was seen with the C_P data of Grigor'ev et al. [83] in the liquid phase. The calculated values for the vapor phase C_P data reported by Mathews and McKetta [84] and by Sinke and Vries [85] deviate from experiment by 4
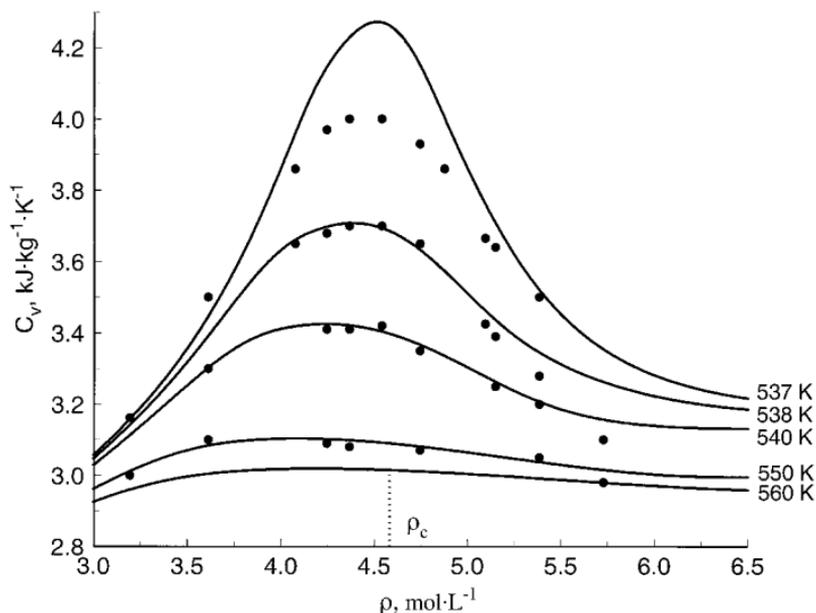
Fig. 4. Experimental one-phase isochoric heat capacity of propan-1-ol [76] (symbols) as a function of density along supercritical isotherms together with values calculated with CR SAFT EOS (lines).
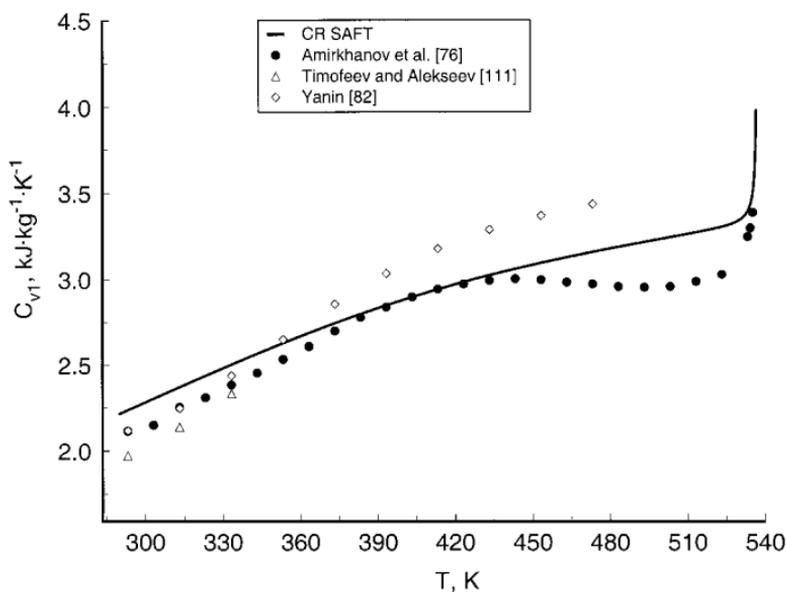
Fig. 5. Experimental liquid one-phase isochoric heat capacity of propan-1-ol as a function of temperature along the coexistence curve together with values calculated with CR SAFT EOS.
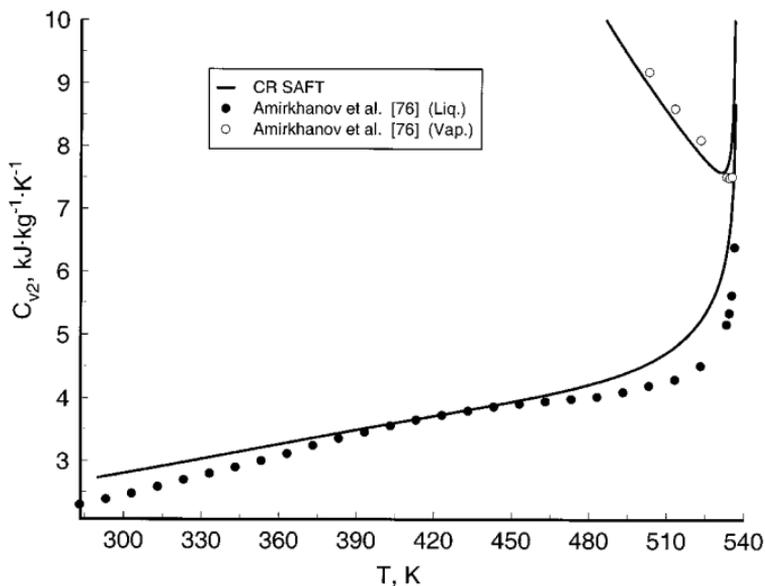
Fig. 6. Experimental liquid and vapor two-phase isochoric heat capacities of propan-1-ol as a function of temperature along the coexistence curve together with values calculated with CR SAFT EOS.
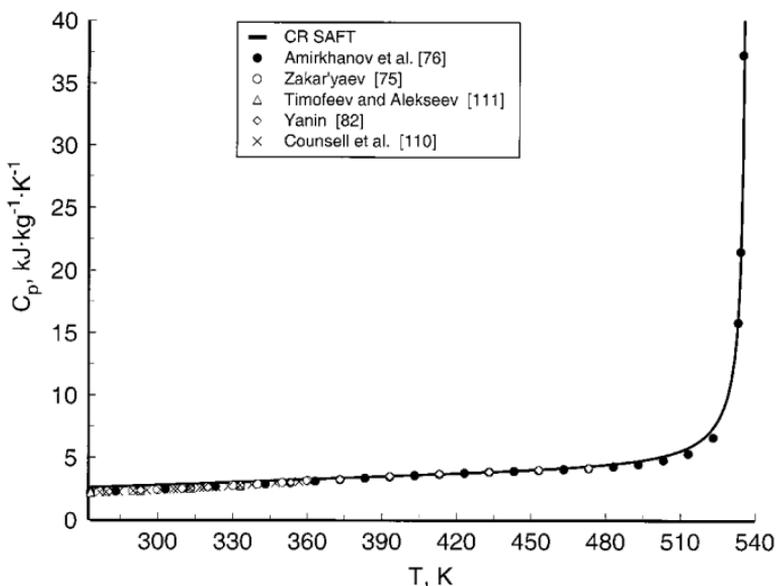
Fig. 7. Experimental isobaric heat capacity of propan-1-ol as a function of temperature along the coexistence curve together with values calculated with CR SAFT EOS.

to 5%. To illustrate how well the model can predict C_P data on the saturation curve, both the calculated values and the available experimental C_P data are compared in Fig. 7. In the temperature range from 370 to 480 K, the agreement between experimental and calculated values of C_P is good (within $\pm 3.0\%$). At lower temperatures ($T < 370$ K), the deviation between measured and calculated data reaches 6% where the calculated values of C_P are systematically high.

Recently Wormald and Vine [119] reported measurements of the specific enthalpy increments $\Delta h = h(P_1, T) - h(P_S, 298$ K$)$ for propan-1-ol, with a standard state $h(P_S, 298.15$ K$) = 0$. Since at low temperatures the CR SAFT EOS is not as accurate as at higher temperatures, the values of the specific enthalpy increments calculated from the model with the same standard state lie about 6–8% higher than the experimental values. If we choose our reference state to be $h(P_S, 298.15$ K$) = -35$ kJ $\cdot$ kg^{-1}, good agreement between calculated values and experimental values is observed as shown in Fig. 8.

Figures 9 and 10 show comparisons between measured and calculated values of sound velocity data for propan-1-ol along vapor–liquid saturated curves and at atmospheric pressure. Deviation plots are given in Figs. 11 and 12. The sound velocity data derived by Amirkhanov et al. [76] from C_V measurements show deviations within 5%. Only at temperatures close
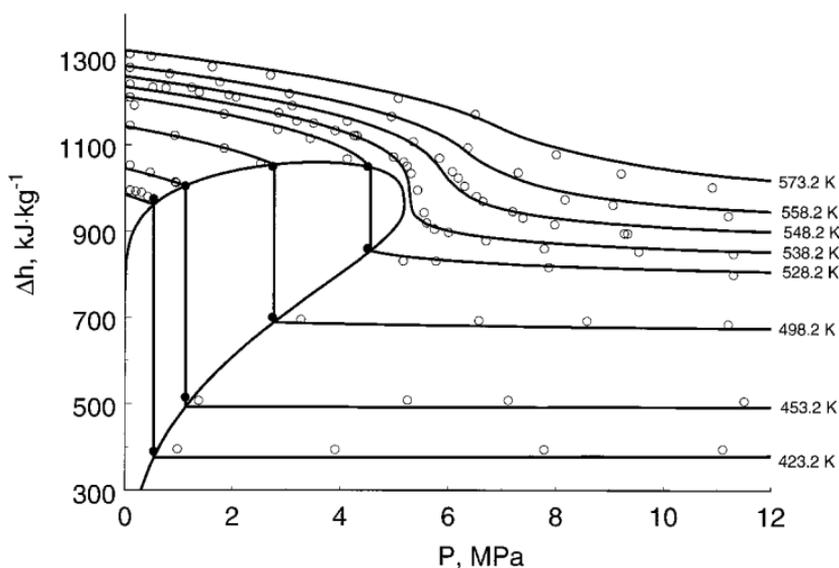
Fig. 8. Specific enthalpy increment as function of pressure along isotherms. The symbols represent experimental data obtained by Wormald and Vine [119] and the curves correspond to values calculated with the CR SAFT EOS with $h(P_S, 298.15$ K$) = -35$ kJ $\cdot$ kg^{-1}.
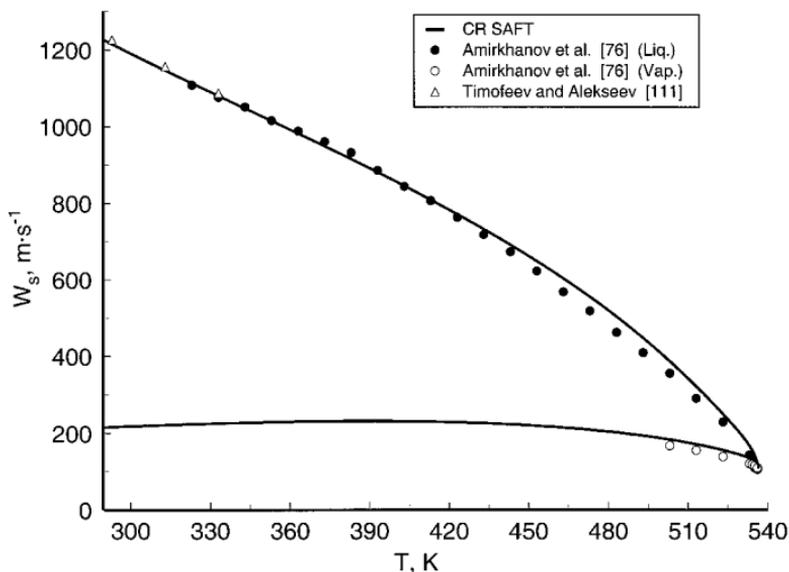
Fig. 9. Experimental sound velocity of propan-1-ol as a function of temperature along the coexistence curve together with values predicted with CR SAFT EOS.
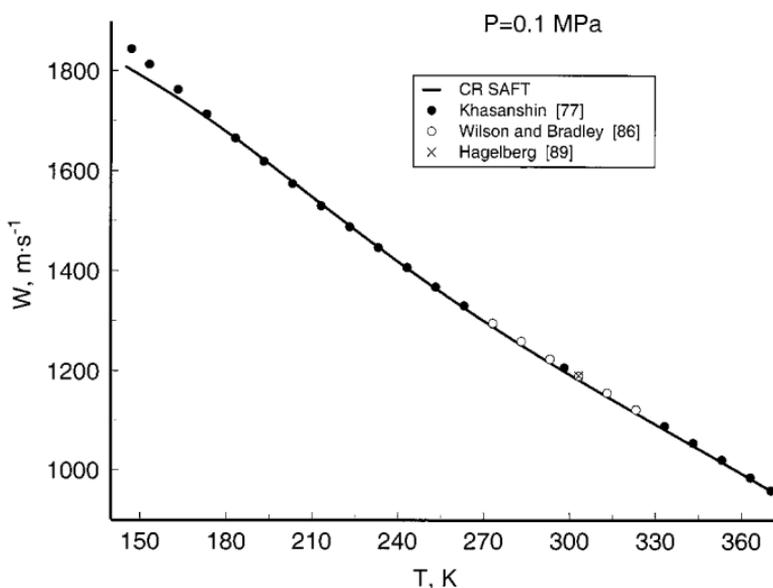
Fig. 10. Experimental sound velocity of propan-1-ol as a function of temperature at atmospheric pressure together with values predicted with CR SAFT EOS.
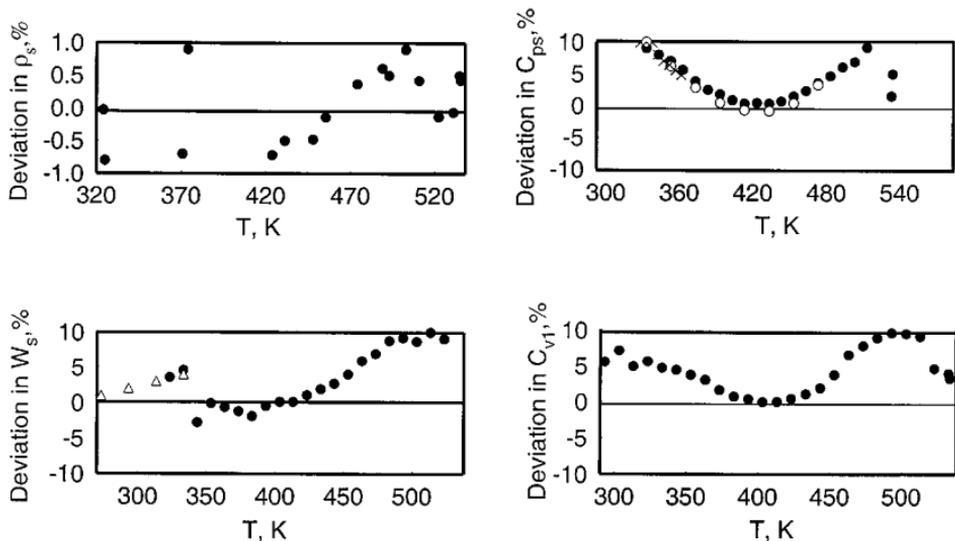
Fig. 11. Percentage deviations of thermodynamic properties of propan-1-ol at saturation from the values calculated with CR SAFT EOS. ●, Amirkhanov et al. [76]; ○, Yanin [82]; ×, Counsell et al. [110]; △, Timofeev and Alekseev [111].
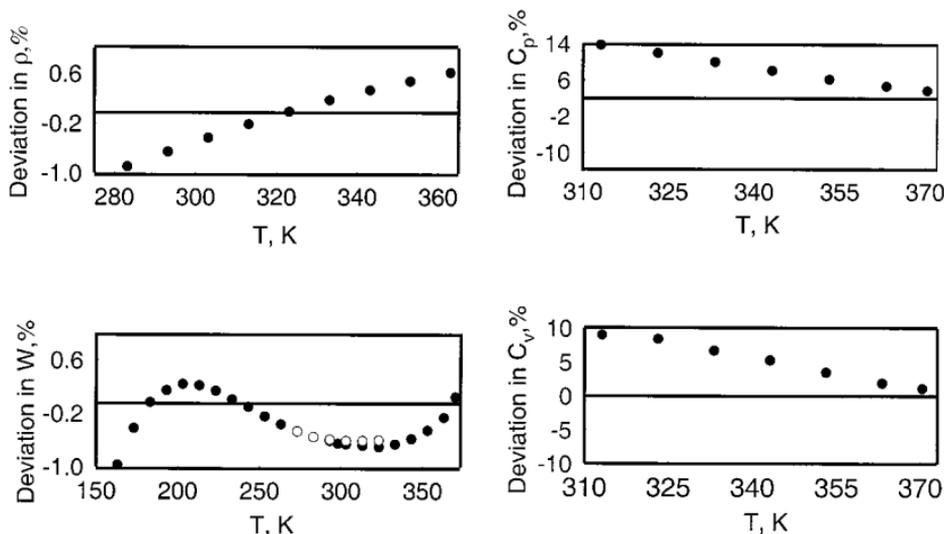
Fig. 12. Percentage deviations of thermodynamic properties of propan-1-ol at atmospheric pressure recommended by (●) Khasanshin [77] and experimental sound velocity data from (○) Wilson and Bradley [86] from the values predicted with CR SAFT EOS.

to the critical point ($T > 500$ K) do the deviations reach as much as 10%. Deviations less than $\pm 0.5\%$ were observed for the Khasanshin [77] data at atmospheric pressure, except for one experimental data point at a low temperature (160 K). Measurements by Wilson and Bradley [86] at atmospheric pressure show small systematic deviations from values calculated by CR SAFT of about 0.5%. Small systematic deviations of about 0.75% were also found for the Timofeev and Alekseev [111] measurements along the saturation curve.

Comparisons of the model calculations with all available experimental liquid and vapor saturated density data are shown in Fig. 13 in the temperature range from room temperature up to the critical point. The deviation statistics for the primary (judged to be more accurate) data sets are given in Table IV, and a deviation plot for these is shown in Fig. 14. As mentioned earlier, the most sensitive test of consistency of saturated density data is a test of the rectilinear diameter as a function of temperature. As discussed above (see Fig. 1), the data of Loktev [80] and Martin et al. [104] near the critical point are inconsistent with other data and fail to reproduce correctly the singular behavior of the diameter. The crossover
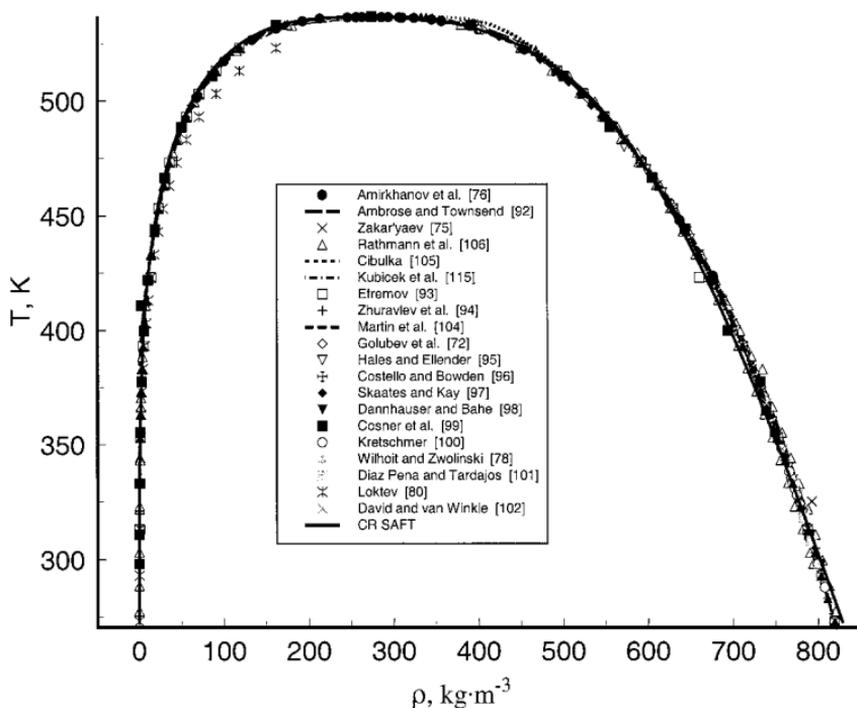
Fig. 13. Experimental liquid and vapor saturated densities of propan-1-ol together with values calculated with CR SAFT EOS and with correlation equations.

Table IV. Deviation Statistics for Saturation Densities

	Ref. No.							
	104	115	106	105	80	92	95	72
AAD (%)	0.36	0.2	0.38	0.18	0.24	0.54	0.97	0.56
Bias (%)	−0.10	0.08	−0.38	0.06	−0.14	−0.54	0.62	0.03
SD	0.62	0.29	0.26	0.23	0.27	0.61	1.03	0.69
SE	0.17	0.07	0.07	0.05	0.06	0.14	0.26	0.21

SAFT EOS in the temperature range $300\,\text{K} \leqslant T \leqslant T_c$ qualitatively and quantitatively is in good agreement with saturated density data.

6. CRITICAL AMPLITUDE RATIOS

According to the fluctuation theory of phase transitions [23, 24], asymptotically close to the critical point, the singular part of the isochoric heat capacity $\Delta \bar{C}_V = (T_c/P_c v_c)(C_V - C_V^{reg}) = -(1/Z_c)(\partial^2 \Delta \bar{A}/\partial \tau^2)_V$ and susceptibility $\bar{\chi}_T = P_c(\partial \Delta \eta/\partial P)_T$ along the critical isochore, the external field $\Delta \bar{P} = (P - P_c)/P_c = -(1/Z_c)(\partial \Delta \bar{A}/\partial \Delta \eta)_T$ along the critical isotherm, and the order parameter at the coexistence curve $\Delta \eta_{lv} = (\Delta \eta_l - \Delta \eta_v)/2$ satisfy the following power laws:

$$\Delta \bar{C}_V = A_0^+ \tau^{-\alpha}(1 + A_1 \tau^{\Delta_1}), \qquad \bar{\chi}_T = \Gamma_0^+ \tau^{-\gamma}(1 + \Gamma_1 \tau^{\Delta_1}) \qquad (23)$$

$$\Delta \bar{P} = \pm D_0 |\Delta \eta|^{\delta} (1 + D_1 |\Delta \eta|^{\Delta_1}), \qquad \Delta \eta_{lv} = B_0 |\tau|^{\beta} (1 + B_1 |\tau|^{\Delta_1}) \qquad (24)$$
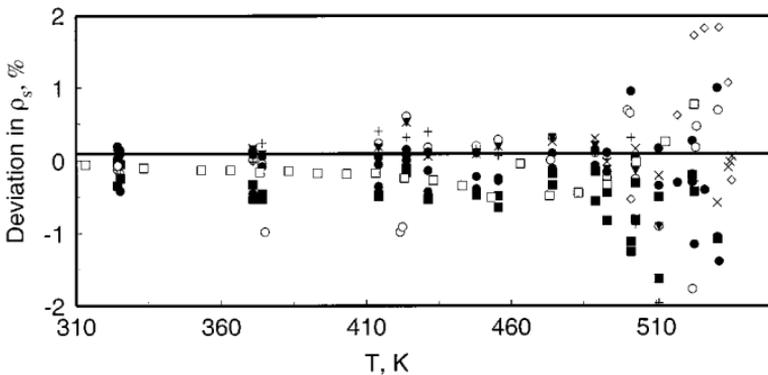
Fig. 14. Percentage deviations of various data sets for saturated densities of propan-1-ol from the values calculated by CR SAFT EOS. ● [115]; □ [80]; × [105]; ◇ [76]; ○ [72]; ■ [106]; ▼ [95]; + [104].

where $\delta = (\gamma + \beta)/\beta$ is a universal critical exponent and the subscripts 0 and 1 correspond to the asymptotic and the first Wegner correction terms, respectively. The critical amplitudes (leading constants) in Eqs. (23) and (24) depend on the intermolecular interactions in the system and are not universal. However, according to theory, the critical amplitude ratios $A_0^+ \Gamma_0^+ / B_0^2$ and $\Gamma_0^+ D_0 B_0^{\delta-1}$ do not depend on the intermolecular interactions and are universal constants [23, 24].

The crossover SAFT EOS does reproduce the asymptotic scaling laws as given by Eq. (24) in the limit $\tau \to 0$. In Fig. 15 we show a comparison between experimental data for the singular part of the isochoric heat capacity for propan-1-ol with the values calculated with the CR SAFT EOS. Excellent agreement between experimental data and predicted asymptotic behavior is observed. However, to check a universality of the critical amplitude ratios for the crossover SAFT EOS, one needs the analytical expressions for the critical amplitudes A_0^+, Γ_0^+, D_0, and B_0 as functions of all system-dependent parameters of the model (see Table II). Unfortunately, the critical parameters of the SAFT EOS T_{0c} and v_{0c}, which are directly related to the asymptotic amplitudes A_0^+, Γ_0^+, D_0, and B_0, can only be obtained from numerical solution of Eq. (10). Therefore, except for the amplitude A_0^+, all other amplitudes in Eqs. (23) and (24) cannot be expressed as analytical functions of the parameters m, v^{00}, u^0, ε^{AB}, and κ^{AB},
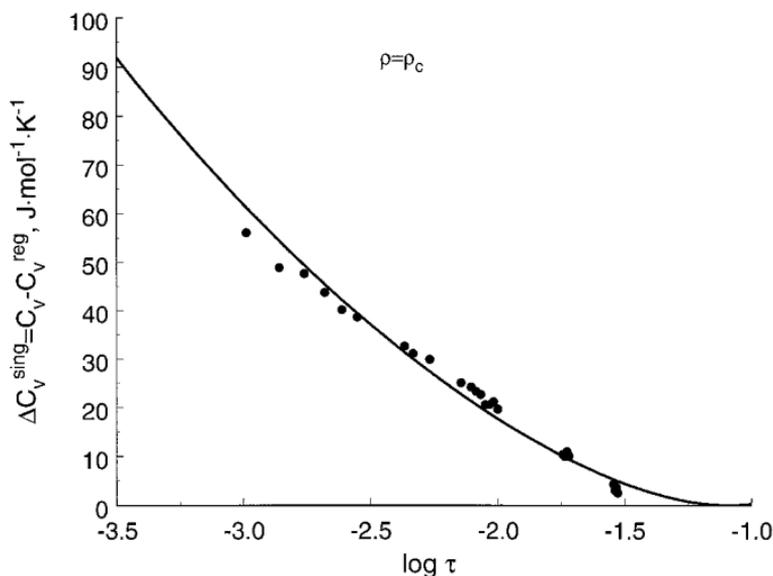
Fig. 15. Singular part of the isochoric heat capacity of propan-1-ol along the critical isochore as a function of τ. The solid curve represents the values calculated with the CR SAFT EOS and the symbols represent the experimental data [76].

and the universality of the critical amplitude ratios cannot be established in general. We can only check how the CR SAFT EOS with parameters given in Table II matches the universal values of these amplitude ratios.

Since the singularity of the isochoric heat capacity along the critical isochore is directly related to the kernel term, $\Delta \bar{C}_V(\tau, \Delta \eta = 0) = (1/Z_c)(\partial^2 K/\partial \tau^2)_{V=V_c}$, one can obtain from Eq. (17)

$$A_0^+ = \frac{(2-\alpha)(1-\alpha)}{2Z_c} a_{20} Gi^\alpha \tag{25}$$

With the parameters a_{20} and Gi given in Table II, Eq. (25) yields $A_0^+ = 53.0$. All other asymptotic critical amplitudes for propan-1-ol have been obtained from a fit of Eqs. (23) and (24) to the $\bar{\chi}_T$, $\Delta \bar{P}$, and $\Delta \eta_{lv}$ data generated in the critical region with the crossover SAFT EOS. Since, in general, the values of the critical amplitudes obtained this way depend on the temperature or density range where they have been found, we considered them in the limit $\tau \to 0$ (or $\Delta \eta \to 0$ for D_0). The amplitudes $\Gamma_0^+ = 0.0247$ and $D_0 = 17.3$ were found with a high precision, since they correspond to the quantities calculated in the one-phase region where the corresponding data can be generated extremely close to the critical point, i.e., with temperatures $\tau \approx 10^{-7}$ to 10^{-9}. The amplitude B_0 determines an asymptotic singular behavior of the coexistence curve, which in turn can be found only from numerical solution of transcendental algebraic equations. This solution
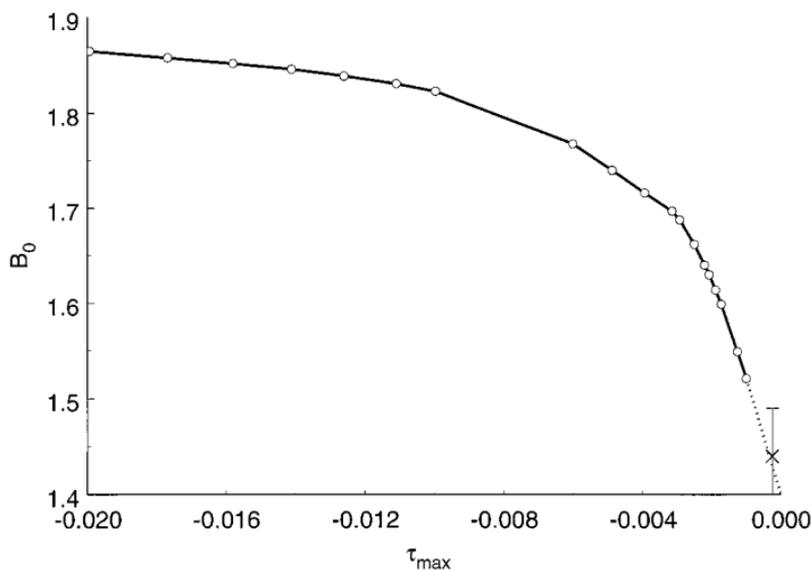
Fig. 16. Asymptotic critical amplitude B_0 for propan-1-ol as a function of the temperature interval $|\tau_{max}|$ where it has been found.

Table V. Values for the Critical Amplitude Ratios

Amplitude ratio	CR SAFT EOS propan-1-ol	Experimental value [133]	Theoretical values		
$\alpha A_0^+ \Gamma_0^+ / B_0^2$	0.069 ± 0.002	0.088 ± 0.040	0.066 [134]	0.059 [135]	0.058 [136]
$D_0 \Gamma_0^+ B_0^{\delta-1}$	1.71 ± 0.10	1.75 ± 0.30	1.66 [134]	1.70 [137]	1.57 [136]

becomes unstable as the critical point is approached (at $|\tau| < 10^{-5}$). Therefore, the value of the critical amplitude $B_0 = 1.44 \pm 0.05$ was found from graphical extrapolations of results obtained at $|\tau_{max}| \geqslant 10^{-5}$ (see Fig. 16). The values for the critical amplitude ratios for propan-1-ol calculated with these amplitudes, together with experimental values obtained by other investigators for different fluids and with the theoretical values, are given in Table V. Reasonably good agreement between theoretical and our values of the critical amplitude ratios is observed, indicating that our CR SAFT EOS for propan-1-ol is thermodynamically consistent with the fundamental results of the modern theory of phase transitions and critical phenomena.

7. DISCUSSION AND EXTENSION TO OTHER FLUIDS

We have developed a crossover SAFT equation of state for propan-1-ol, which reproduces the nonanalytical scaling laws asymptotically close to the critical point and reduces to the analytical-classical SAFT EOS far away from the critical point. The CR SAFT EOS for propan-1-ol contains 10 system-dependent parameters and gives a very good representation the heat capacities, speed of sound, PVT, and VLE data over a wide range of thermodynamic states including the asymptotic singular behavior in the nearest vicinity of the critical point. Some problems arise at low temperatures and densities where deviations of the calculated values of the isochoric and isobaric heat capacities from experimental data increase up to 15 to 18%. At low densities, $\rho \to 0$ and $P \to 0$, the heat capacities C_V and C_P are determined by the second virial coefficients b_2 (or b_2^P for C_P) [120]

$$\left(\frac{\partial C_V}{\partial v}\right)_T = T \left(\frac{\partial^2 P}{\partial T^2}\right)_V \cong \rho RT \left[\left(2\frac{db_2}{dT} + T\frac{d^2 b_2}{dT^2} \right) \rho + O(\rho^2) \right] \quad (26)$$

$$\left(\frac{\partial C_P}{\partial P}\right)_T = -T \left(\frac{\partial^2 v}{\partial T^2}\right)_P \cong -\frac{RT}{P} \left[\left(2\frac{db_2^P}{dT} + T\frac{d^2 b_2^P}{dT^2} \right) P + O(P^2) \right] \quad (27)$$

and it is well known that the original SAFT EOS which is based on statistical mechanical perturbation theory does not reproduce the correct temperature dependence of the second virial coefficient at temperatures where $u/(kT) \geqslant 1$. Thus, to improve the representation of experimental data with the crossover SAFT EOS in this region, the original SAFT EOS should be improved first. However, even in its present form the CR SAFT EOS yields a very good representation of the thermodynamic properties of propan-1-ol in a wide range of densities for $T \geqslant 250$ K [where $(u/kT) \leqslant 0.7$], and also allows extrapolations of these results to higher n-alkanols.

In Fig. 17 we show a comparison of the saturated pressures and densities calculated with a simple corresponding-states (CS) model

$$P_{sat}^{X}(T) = P_{sat}^{C3}\left(T\,\frac{T_c^X}{T_c^{C3}} \right)\frac{P_c^X}{P_c^{C3}}, \qquad \rho_{sat}^{X}(T) = \rho_{sat}^{C3}\left(T\,\frac{T_c^X}{T_c^{C3}} \right)\frac{\rho_c^X}{\rho_c^{C3}} \qquad (28)$$

where the superscript $C3$ corresponds to the propan-1-ol reference fluid, and the superscript X to the target fluids which in this case are higher molecular weight n-alkanols $C4$, $C5$,..., etc. As one can see, up to octanol,
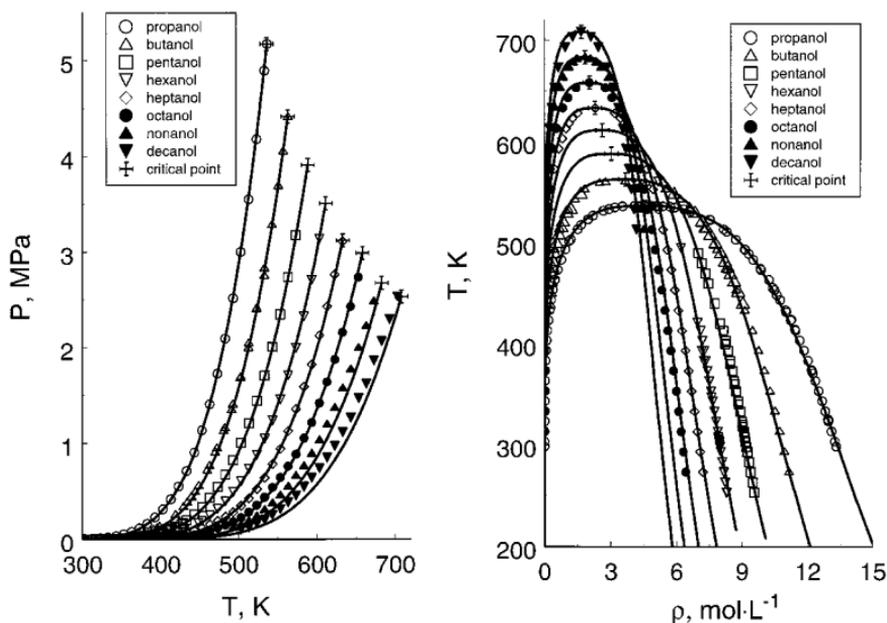
Fig. 17. Saturated pressure (left) and saturated density (right) data for propan-1-ol [115, 117], butan-1-ol [92, 93, 117, 130], pentan-1-ol [78, 95, 138, 139], hexan-1-ol [78, 138-140], heptan-1-ol [132], and octan-1-ol, nonan-1-ol, and decan-1-ol [93] (symbols) with corresponding states predictions (lines).

reasonably good agreement between the CS model and experimental values of the saturated pressures and densities is observed. Starting from *n*-nonanol, systematic deviations of the calculated values of pressures and densities from the experimental values are seen. There are two fundamental reasons for this behavior. First, the deviations of saturated pressures are the result of the fact that the slope of the vapor pressure curve at the critical point for *n*-nonanol and *n*-decanol differs substantially from that for propan-1-ol. In principle, these deviations can be corrected by incorporating the acentric factor ω into Eqs. (28). However, the deviations of the saturated densities cannot be corrected by this modification. In Fig. 18 we show the saturated densities for *n*-alkanols in the dimensionless coordinates, $\tau - \Delta\rho$. The dashed curve in Fig. 18 represents the values calculated with the mean-field expression

$$\Delta\rho_{cxs} = \frac{\rho_{l,g} - \rho_c}{\rho_c} = \pm\hat{B}_0\,|\tau|^{0.5} - \hat{B}_3\tau \tag{29}$$

with the mean-field critical amplitudes $\hat{B}_0 = 3.0$ and $\hat{B}_3 = 0.9$. Excellent agreement with experimental data for *n*-decanol is observed in this case. This suggests that with increasing molecular weight, a crossover from non-analytic ($\beta = 0.325$) to mean-field ($\beta = 0.5$) behavior takes place. This observation is consistent with Lue and Friend's general analysis of the
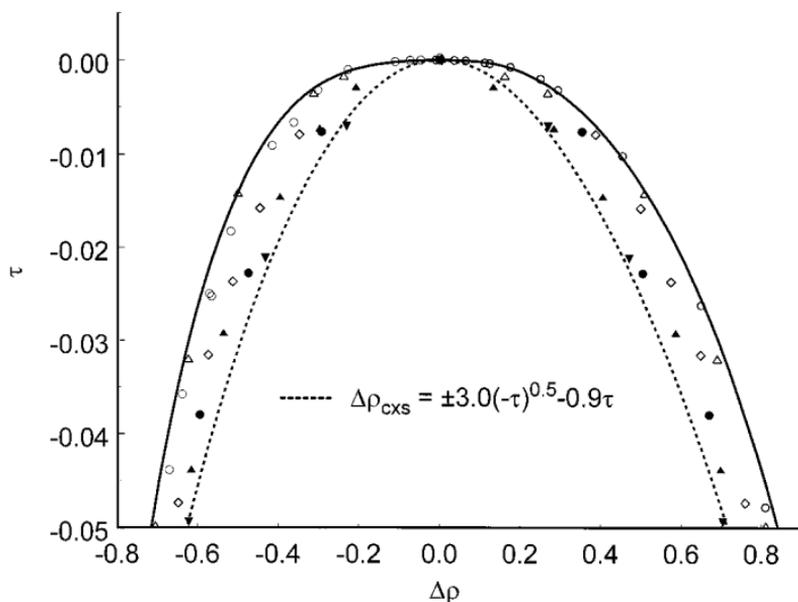
Fig. 18. Saturated densities for *n*-alkanols in the dimensionless coordinates. See legend to Fig. 17.

SAFT-type EOS [121], which indicates that a crossover from scaling to classical, or mean-field, behavior should appear with an increase in the molecular weight. The crossover behavior of saturated densities can be taken into account by incorporating the Ginzburg number Gi in Eqs. (28). The development of this new crossover modification of the CS principle for *n*-alkanols and other fluids is now in progress, and the results of this study will be reported in a future publication.

ACKNOWLEDGMENTS

REFERENCES

1. J. D. van der Waals and F. Kohnstamm, *Lehrbuch der Thermostatic*, 2er Teil (Verlag von Johann Amrosius Barth, Leipzing, 1927).
2. O. Redlich and J. N. S. Kwong, *Chem. Rev.* **44**:233 (1949).
3. G. Soave, *Chem. Eng. Sci.* **27**:1197 (1972).
4. D. Y. Peng and D. B. Robinson, *Ind. Eng. Chem. Fundam.* **15**:58 (1976).
5. N. C. Patel and A. S. Teja, *Chem. Eng. Sci.* **37**:463 (1982).
6. A. Peneloux and E. Rauzy, *Fluid Phase Equil.* **8**:7 (1982).
7. R. Solimando, E. Rogalski, E. Neau, and A. Peneloux, *Fluid Phase Equil.* **106**:59 (1995).
8. E. Behar, R. Simonet, and E. Rauzy, *Fluid Phase Equil.* **21**:237 (1985).
9. P. M. Mathias, T. Naheiri, and E. M. Oh, *Fluid Phase Equil.* **47**:77 (1989).
10. S. M. Walas, *Phase Equilibrium in Chemical Engineering* (Butterworths, Boston, 1985).
11. C. R. Reid, J. M. Prausnitz, and B. E. Polling, *The Properties of Gases and Liquids*, 4th ed. (McGraw–Hill, New York, 1987).
12. Y. H. Song, S. M. Lambert, and J. M. Prausnitz, *Ind. Eng. Chem. Res.* **33**:1047 (1994).
13. Y. H. Song, S. M. Lambert, and J. M. Prausnitz, *Chem. Eng. Sci.* **49**:2765 (1994).
14. Y. Hu, L. Lue, and J. M. Prausnitz, *J. Chem. Phys.* **104**:396 (1996).
15. T. Hino and J. M. Prausnitz, *Fluid Phase Equil.* **138**:105 (1997).
16. W. G. Chapman, K. E. Gubbins, G. Jackson, and M. Radosz, *Fluid Phase Equil.* **52**:31 (1989).
17. S. H. Huang and M. Radosz, *Ind. Eng. Chem. Res.* **29**:2284 (1990).
18. S. H. Huang and M. Radosz, *Ind. Eng. Chem. Res.* **30**:1994 (1991).
19. M. Banaszak, Y. C. Chiew, and M. Radosz, *Phys. Rev. E* **48**:3760 (1993).
20. M. Banaszak, Y. C. Chiew, R. O'Lenick, and M. Radosz, *J. Chem. Phys.* **100**:3803 (1994).
21. H. Adidharma and M. Radosz, *Fluid Phase Equil.* **161**:1 (1999).

22. R. T. Jacobsen, S. G. Penoncello, E. W. Lemmon, and R. Span, in *Equations of State for Fluids and Fluid Mixtures*, J. V. Sengers, R. F. Kayser, C. J. Peters, and H. J. White, Jr., eds. (Elsevier, Amsterdam, 2000)

23. A. Z. Patashinskii and V. L. Pokrovskii, *Fluctuation Theory of Phase Transitions*, 3rd ed. (Pergamon, New York, 1979).

24. M. E. Fisher, *Critical Phenomena*, Lecture Notes in Physics, Vol. 186, J. W. Hanhne, ed. (Springer-Verlag, Berlin, 1982).

25. M. A. Anisimov, S. B. Kiselev, J. V. Sengers, and S. Tang, *Physica A* **188**:487 (1992).

26. Z. Y. Chen, A. Abbaci, S. Tang, and J. V. Sengers, *Phys. Rev. A* **42**:4470 (1990).

27. Z. Y. Chen, P. C. Albright, and J. V. Sengers, *Phys. Rev. A* **41**:3161 (1990).

28. G. X. Jin, S. Tang, and J. V. Sengers, *Fluid Phase Equil.* **75**:1 (1992).

29. G. X. Jin, S. Tang, and J. V. Sengers, *Phys. Rev. E* **47**:388 (1993).

30. A. A. Povodyrev, G. X. Jin, S. B. Kiselev, and J. V. Sengers, *Int. J. Thermophys.* **17**:909 (1996).

31. A. Kostrowicka-Wyczalkowska and J. V. Sengers, *J. Chem. Phys.* **111**:1551 (1999).

32. S. B. Kiselev, I. G. Kostyukova, and A. A. Povodyrev, *Int. J. Thermophys.* **12**:877 (1990).

33. S. B. Kiselev, *High Temp.* **28**:47 (1990).

34. S. B. Kiselev and J. V. Sengers, *Int. J. Thermophys.* **14**:1 (1993).

35. S. B. Kiselev, *Fluid Phase Equil.* **128**:1 (1997).

36. S. B. Kiselev and J. C. Rainwater, *Fluid Phase Equil.* **141**:129 (1997).

37. S. B. Kiselev, J. C. Rainwater, and M. L. Huber, *Fluid Phase Equil.* **150**:469 (1998).

38. S. B. Kiselev, M. Y. Belyakov, and J. C. Rainwater, *Fluid Phase Equil.* **150**:439 (1998).

39. S. B. Kiselev and J. C. Rainwater, *J. Chem. Phys.* **109**:643 (1998).

40. S. B. Kiselev and M. L. Huber, *Int. J. Refrig.* **21**:64 (1998).

41. S. B. Kiselev, M. Abdulagatov, and A. H. Harvey, *Int. J. Thermophys.* **20**:563 (1999).

42. M. Y. Belyakov, S. B. Kiselev, and J. C. Rainwater, *J. Chem. Phys.* **107**:3085 (1997).

43. J. R. Fox, *Fluid Phase Equil.* **14**:45 (1983).

44. A. Parola and L. Reatto, *Phys. Rev. Lett.* **53**:2417 (1984).

45. A. Parola and L. Reatto, *Phys. Rev. A* **31**:3309 (1985).

46. A. Parola, A. Meroni, and L. Reatto, *Int. J. Thermophys.* **10**:345 (1989).

47. M. Tau, A. Parola, D. Pini, and L. Reatto, *Phys. Rev. E* **52**:2644 (1995).

48. L. Reatto and A. Parola, *J. Phys. Condens. Matter* **8**:9221 (1996).

49. P. C. Albright, J. V. Sengers, J. F. Nicoll, and M. Ley-Koo, *Int. J. Thermophys.* **7**:75 (1986).

50. A. Kostrowichka-Wyczalkovska, M. A. Anisimov, and J. V. Sengers, *Fluid Phase Equil.* **158**–**160**:523 (1999).

51. A. van Pelt, G. X. Jin, and J. V. Sengers, *Int. J. Thermophys.* **15**:687 (1994).

52. D. D. Erikson and T. W. Leland, *Int. J. Thermohys.* **7**:911 (1986).

53. J. J. De Pablo and J. M. Prausnitz, *Fluid Phase Equil.* **59**:1 (1990).

54. T. Kraska and U. K. Deiters, *Int. J. Thermophys.* **15**:261 (1993).

55. J. A. White and S. Zhang, *J. Chem. Phys.* **103**:1922 (1990).

56. J. A. White and S. Zhang, *J. Chem. Phys.* **99**:2012 (1993).

57. J. A. White, *J. Chem. Phys.* **111**:9352 (1999).

58. J. A. White, *J. Chem. Phys.* **112**:3236 (2000).

59. L. Lue and J. M. Prausitz, *J. Chem. Phys.* **108**:5529 (1998).

60. L. Lue and J. M. Prausitz, *AICHE J.* **44**:1455 (1998).

61. F. Fornasiero, L. Lue, and A. Bertucco, *AIChE J.* **45**, in press.

62. J. Jiang and J. M. Prausnitz, *J. Chem. Phys.* **111**:5964 (1999).

63. S. B. Kiselev, *Fluid Phase Equil.* **147**:7 (1998).

64. S. B. Kiselev and D. G. Friend, *Fluid Phase Equil.* **162**:51 (1999).

65. S. B. Kiselev and J. F. Ely, *Ind. Eng. Chem. Res.* **38**:4993 (1999).
66. S. B. Kiselev and J. F. Ely, *Fluid Phase Equil.* **174**:93 (2000).
67. S. B. Kiselev, J. F. Ely, H. Adidharma, and M. Radosz, *Fluid Phase Equil.* (in press).
68. S. S. Chen and A. Kreglewski, *Ber. Bunsen-Ges. Phys. Chem.* **81**:1048 (1977).
69. S. B. Kiselev and D. G. Friend, *Fluid Phase Equil.* **155**:33 (1999).
70. M. Fisher, S.-Y. Zinn, and P. Upton, *Phys. Rev. B* **59**:14533 (1999).
71. W. Ramsay and S. Young, *Phil. Trans. Roy. Soc. London A* **180**:137 (1889).
72. I. F. Golubev, T. N. Vasil'kovskaya, and B. C. Zolin, *Trudy GIAP* **54**:5 (1979).
73. I. F. Golubev and E. N. Bagina, *Trudy GIAP* **15**:39 (1963).
74. J. Tseng and L. Stiel, *AIChE J.* **17**:1283 (1971).
75. Z. R. Zakar'yaev, Ph.D. thesis (Institute for Geothermal Reaserch, Makhachkala, 1996).
76. K. I. Amirkhanov, G. V. Stepanov, I. M. Abdulagatov, and O. A. Byoi, *Isochoric Heat Capacity of Propan-1-ol and Propan-2-ol*, V. V.Sychev, ed. (Dagestan Scientific Center of the Russian Academy of Sciences, Makhachkla, 1989).
77. T. S. Khasanshin, *Russ. Phys. Eng. J.* **45**:461 (1983).
78. R. C. Wilhoit and B. J. Zwolinski, *J. Phys. Chem. Ref. Data* **2**:Suppl. 1 (1973).
79. G. S. Parks and H. M. Huffman, *J. Am. Chem. Soc.* **48**:2788 (1926).
80. S. M. Loktev, *Vysshie zhirnye spirty* (Khimiya, Moscow, 1970).
81. J.-L. Fortier, G. C. Benson, and P. Picker, *J. Chem. Thermodyn.* **8**:289 (1976).
82. G. S. Yanin, Ph.D. thesis (Groznyi Oil Institute, Groznyi, 1977)
83. B. A. Grigor'ev, G. S. Yanin, and Y. L. Rastorguev, *Trudy GIAP* **54**:57 (1979).
84. J. F. Mathews and J. J. McKetta, *J. Phys. Chem.* **65**:758 (1961).
85. G. C. Sinke and T. Vries, *J. Am. Chem. Soc.* **75**:1815 (1953).
86. W. Wilson and D. Bradley, *J. Acoust. Soc. Am.* **36**:333 (1964).
87. J. Emery, S. Gasse, R. A. Pethrick, and D. W. Phillips, *Adv. Mol. Relax. Int. Proc.* **12**:47 (1978).
88. S. Gasse and J. Emery, *J. Chem. Phys.* **77**:263 (1980).
89. M. P. Hagelberg, *J. Acoust. Soc. Am.* **47**:158 (1970).
90. E. H. Carnevale and T. A. Litovitz, *J. Acoust. Soc. Am.* **27**:547 (1955).
91. I. V. Sysoev, N. F. Otpushennikov, and Y. S. Shoitov, *Ultrazvuk I Fiz.-Khim. Svoistva Veshestv* **11**:102 (1977).
92. D. Ambrose and R. Townsend, *J. Chem. Soc.* **37**:3614 (1963).
93. Y. V. Efremov, *Russ. J. Phys. Chem.* **40**:1240 (1966).
94. V. I. Zhuravlev, V. A. Durov, T. M. Usacheva, and M. I. Shaxporonov, *Russ. J. Phys. Chem.* **59**:1677 (1985).
95. J. L. Hales and J. H. Ellender, *J. Chem. Thermodyn.* **8**:1177 (1976).
96. J. M. Costello and S. T. Bowden, *Rec. Trav. Chim. Pays-Bas.* **77**:36 (1958).
97. J. M. Skaates and W. B. Kay, *Chem. Eng. Sci.* **19**:431 (1964).
98. W. Dannhauser and L. W. Bahe, *J. Chem. Phys.* **40**:3058 (1964).
99. J. L. Cosner, J. E. Gagliardo, and T. S. Storvick, *J. Chem. Eng. Data* **6**:360 (1961).
100. C. B. Kretschmer, *J. Phys. Chem.* **55**:1351 (1951).
101. M. Diaz Pena and G. Tardajos, *J. Chem. Thermodyn.* **11**:441 (1979).
102. T. David and M. van Winkle, *Ind. Eng. Chem.* **3**:88 (1958).
103. S. Z. Young, *Physik. Chem. (Leipzig)* **70**:620 (1910).
104. J. J. Martin, J. A. Campbell, and E. M. Seidel, *J. Chem. Eng. Data* **8**:560 (1963).
105. I. Cibulka, *Fluid Phase Equil.* **89**:1 (1993).
106. D. Rathmann, D. A. Sullivan, and P. A. Thompson, *Liquid–Vapor Saturation Density Data* (Max-Planck Institute für Strömungsforschung, Göttingen, 1979), p. 52.
107. D. P. Biddiscombe, R. R. Collerson, R. Handley, E. F. G. Herington, J. F. Martin, and C. H. S. Sparke, *J. Chem. Soc.* **37**:1954 (1963).

108. D. Ambrose and J. Walton, *Pure Appl. Chem.* **61**:1395 (1989).
109. *Vapor Pressure and Critical Properties of Liquids*, *Alkanols*, *Data Items 88005*, *88012* (ESDU International, London, 1988).
110. J. F. Counsell, E. B. Lees, and J. F. Martin, *J. Chem. Soc. A* **8**:1819 (1968).
111. N. E. Timofeev and V. V. Alekseev, *Ultrazvuk I Fiz.-Khim. Svoistva Veshestv* **11**:142 (1983).
112. D. Ambrose and R. Townsend, *Correlation and Estimation of Vapor–Liquid Critical Properties*, *Rep. Chem. 92* (National Physical Laboratory, Teddington, 1978).
113. J. F. Nicoll, *Phys. Rev. A* **24**:2203 (1981).
114. W. B. Kay and W. E. Donham, *Chem. Eng. Sci.* **4**:1 (1955).
115. A. J. Kubicek and P. T. Eubank, *J. Chem. Eng. Data* **17**:232 (1972).
116. C. N. Yang and C. P. Yang, *Phys. Rev. Lett.* **13**:303 (1969).
117. D. Ambrose and C. H. Sprake, *J. Chem. Thermodyn.* **2**:631 (1970).
118. I. F. Golubev, T. N. Vasil'kovskaya, and V. S. Zolin, *Inzh.-Fiz. Zh.* **45**:668 (1980).
119. C. J. Wormald and M. D. Vine, *J. Chem. Thermodyn.* **32**:329 (2000).
120. L. D. Landau and E. M. Lifshitz, *Statistical Physics*, *Part 1* (Pergamon Press, New York, 1980).
121. L. Lue and D. G. Friend, *Mol. Phys.* (in press).
122. K. M. Khalilov, *Russ. Exp. Theor. Phys. J.* **9**:335 (1939).
123. R. Fischer and T. Reichel, *Mikrochem. Acta* **31**:102 (1943).
124. A. L. Lyderson, A. R. Greenkorn, and O. A. Hougen, *Generalized Properties of Pure Fluids*, *Eng. Exp. Stat. Rep. 4* (University of Wisconsin, Madison, 1955).
125. P. T. Eubank and J. M. Smith, *J. Chem. Eng. Data* **7**:75 (1962).
126. C. L. Jows and J. R. Hopper, *Chem. Eng.* **83**:119 (1976).
127. K. A. Kobe and R. E. Lynn, *Chem. Rev.* **52**:117 (1953).
128. A. P. Kudchadker, G. H. Alani, and B. J. Zwolinski, *Chem. Rev.* **68**:659 (1968).
129. A. M. Zhuravlev and Y. Z. Kazavchinskii, *Russ. J. Phys. Chem.* **37**:181 (1963).
130. N. B. Vargaftik, *Tables on the Thermophysical Properties of Liquids and Gases in Normal and Dissociated States*, Vol. 767 (Hemisphere, New York, 1975).
131. R. S. Machado and W.B. Street, *J. Chem. Eng. Data* **28**:218 (1983).
132. K. R. Hall (Thermodynamics Research Center, Texas A&M University, College Station, 1987).
133. M. A. Anisimov and S. B. Kiselev (eds.), *Universal Crossover Approach to Description of Thermodynamic Properties of Fluids and Fluid Mixtures*, Sov. Tech. Rev. B. Therm. Phys., Vol. 3, Part 2, A. E. Scheindlin and V. E. Fortov (eds.) (Harwood Academic, New York, 1992), p. 1.
134. A. Ahorony and P. C. Hohenberg, *Phys. Rev. B* **24**:3081 (1976).
135. C. Bagnuls and C. Bervillier, *Phys. Rev. B* **24**:1226 (1981).
136. A. J. Liu and M. E. Fisher, *Physica A* **156**:35 (1989).
137. J. Zinn-Justin, *J. Phys.* **42**:783 (1981).
138. K. R. Hall (Thermodynamics Research Center, Texas A&M University, College Station, 1980).
139. D. R. Stull, *Ind. Eng. Chem.* **39**:517 (1947).
140. J. Ortega, *J. Chem. Eng. Data* **30**:5 (1985).